1   A natural genetic variation screen identifies insulin signaling, neuronal communication, and

2   innate immunity as modifiers of hyperglycemia in the absence of *Sirt1*

3

4   Rebecca A.S. Palu

5   Biology Department, Purdue University-Fort Wayne, Fort Wayne, IN 46818

6

7

8

9

10

11

12

13

14

15

16   **Running title: Natural modifiers of hyperglycemia**

17   **Key words: hyperglycemia, *Drosophila*, genetic variation, modifier genes**

18

19   Corresponding author:

20   Rebecca A.S. Palu

21   Biology Department

22   Science Building SB330

23   2101 E. Coliseum Blvd

24   Fort Wayne IN, 46805

25   260-481-5704

26   palur@pfw.edu

27 **ABSTRACT**

28 Variation in the onset, progression, and severity of symptoms associated with metabolic

29 disorders such as diabetes impairs the diagnosis and treatment of at-risk patients. Diabetes

30 symptoms, and patient variation in these symptoms, is attributed to a combination of genetic

31 and environmental factors, but identifying the genes and pathways that modify diabetes in

32 humans has proven difficult. A greater understanding of genetic modifiers and the ways in which

33 they interact with metabolic pathways could improve the ability to predict a patient's risk for

34 severe symptoms, as well as enhance the development of individualized therapeutic

35 approaches. In this study we use the *Drosophila* Genetic Reference Panel (DGRP) to identify

36 genetic variation influencing hyperglycemia associated with loss of *Sirt1* function. Through

37 analysis of individual candidate functions, physical interaction networks, and Gene Set

38 Enrichment Analysis (GSEA) we identify not only modifiers involved in canonical glucose

39 metabolism and insulin signaling, but also genes important for neuronal signaling and the innate

40 immune response. Furthermore, reducing the expression of several of these candidates

41 suppressed hyperglycemia, making them ideal candidate therapeutic targets. These analyses

42 showcase the diverse processes contributing to glucose homeostasis and open up several

43 avenues of future investigation.

44

45 **INTRODUCTION**

46 Metabolic diseases, and in particular diabetes, are one of the most pressing health crises in the

47 developed world, with incidences continuing to rise in the last 20 years (CDC 2020). 37.7% of

48 adults in the US are diagnosed as obese and 10.5% as having some form of diabetes, and it is

49 estimated that millions more go undiagnosed (Flegal *et al.* 2016; CDC 2020). What is more, the

50 monetary cost of these disorders to the public has grown to astronomical levels. It is estimated

51 that $237 billion in direct costs and at least $90 billion in indirect costs were spent on healthcare

52 related to diabetes and its various complications in 2017 alone, up ~25% from 2012 (Flegal *et*

53   *al.* 2016). A focused effort has been made to understand both the genetic and environmental

54   contributors to metabolic homeostasis, as well as to the disruption of that homeostasis that

55   leads to disease (Barroso and McCarthy 2019).

56

57   Unfortunately, even identifying these contributors has proven difficult. Metabolic diseases are

58   complex, and the onset, progression, and ultimately the severity of any individual case is

59   dependent upon a myriad of genetic and environmental variables and the ways in which they

60   interact with one another (Queitsch *et al.* 2012; Barroso and McCarthy 2019). Even when there

61   is a strong familial link, phenotypic heterogeneity in disease phenotypes can make it difficult to

62   identify at-risk patients or make accurate prognostic predictions (Udler *et al.* 2019). This is

63   particularly true when it comes to predicting complications of diabetes such as neuropathy,

64   retinopathy, or kidney disease (Barroso and McCarthy 2019; Cabrera *et al.* 2020). Much of this

65   variation is due to inter-individual differences in genetic background, including silent cryptic

66   genetic variation that is revealed upon disease or stress (Queitsch *et al.* 2012; Chow 2016;

67   Barroso and McCarthy 2019).

68

69   One example of this kind of symptom heterogeneity can be observed in disease associated with

70   the deacetylase *SIRT1*. This highly conserved gene was originally identified as a histone

71   deacetylase important in heterochromatin formation in yeast (Shore *et al.* 1984; Ivy *et al.* 1986;

72   Rine and Herskowitz 1987). Since then, SIRT1 and its paralogs (the sirtuins) have been found

73   to have a number of additional targets, many of which are transcription factors and enzymes

74   with key roles in metabolic homeostasis (Brunet *et al.* 2004; Picard *et al.* 2004; Rodgers and

75   Puigserver 2007; Li *et al.* 2007; Yang *et al.* 2009; Palu and Thummel 2016). Importantly, as part

76   of their enzymatic reaction, sirtuins consume the cofactor NAD, which also serves as an

77   electron carrier in central metabolic pathways such as glycolysis and the TCA cycle. Sirtuin

78   enzymatic activity, therefore, is directly linked to the availability of this cofactor and thus is

79   responsive to the energetic state of the cell. This information is then conveyed to the targets,

80   whose acetylation state alters their activity and stability in the cell (Nogueiras *et al.* 2012). With

81   this centralized role in regulating the response of metabolic factors to cellular energy availability,

82   it is unsurprising that variation in *SIRT1* has been linked to, among other things, the

83   development of diabetes (Zillikens *et al.* 2009; Botden *et al.* 2012; Biason-Lauber *et al.* 2013;

84   Zhao *et al.* 2017).

85

86   Elucidating the mechanism behind this link, however, has proven difficult. Loss-of-function and

87   gain-of-function studies in model systems have demonstrated a clear role for SIRT1 in

88   metabolic homeostasis, but the actual impacts on the animals in question have frequently been

89   contradictory (Boutant and Cantó 2014). It is likely that at least some of these contradictory

90   results stem from differences in genetic background between the animals used in the various

91   studies. Understanding the role of this variation and the genes or pathways which modify

92   metabolic disease will enable the development of improved diagnosis, prediction of prognosis,

93   and personalized treatment strategies for patients.

94

95   Model organism tools, such as the *Drosophila* Genetic Reference Panel (DGRP), provide a way

96   to study of the impact of natural genetic variation on diseases such as diabetes (Mackay *et al.*

97   2012; He *et al.* 2014; Ivanov *et al.* 2015; Nelson *et al.* 2016; Jehrke *et al.* 2018; Everman *et al.*

98   2019). The DGRP is a collection of ~200 isogenic strains derived from a wild population, such

99   that each strain represents one wild-derived genome (Mackay *et al.* 2012). The variation in the

100   DGRP is well tolerated under healthy, non-disease conditions and allows for the identification of

101   genetic polymorphisms that are associated with phenotypic variation in models of human

102   disease (Chow and Reiter 2017). Importantly, the availability of full-genome sequence for these

103   strains allows for genome-wide association analyses that link quantitative phenotypes with

104   genetic variation and modifier genes.

105

106   The utility of the DGRP in identifying candidate modifiers of metabolic disease has already been

107   demonstrated numerous times, with screens associated with misfolded insulin, high sugar and

108   high fat feeding, and starvation resistance already documented (Mackay *et al.* 2012; He *et al.*

109   2014; Ivanov *et al.* 2015; Nelson *et al.* 2016; Jehrke *et al.* 2018; Everman *et al.* 2019). While

110   some of these used biochemical assays to precisely measure metabolite levels in flies as a

111   quantitative phenotype for the screen (Nelson *et al.* 2016; Jehrke *et al.* 2018; Everman *et al.*

112   2019), several used more general physiological measurements such as starvation resistance

113   and lifespan (Mackay *et al.* 2012; Ivanov *et al.* 2015). Although effective, the use of this kind of

114   general readout reduces the specificity of the modifiers identified. Many genetic factors impact

115   survival and could lead to a high background signal. The same could be true for otherwise wild-

116   type flies subjected to different environmental conditions, even when more precise assays are

117   used as a quantitative phenotype (Nelson *et al.* 2016). A multitude of pathways and processes

118   impact the response to dietary changes through feeding rate, hormone secretion, anabolism

119   and catabolism rates, and nutrient absorption. Using a specific genetic model of disease and

120   then focusing on a specific phenotype, such as hyperglycemia, may reduce some of the noise

121   and increase specificity of the modifiers identified.

122

123   Furthermore, recent studies using the DGRP have demonstrated that the top candidate modifier

124   genes and pathways differ when different but related models of genetic disease are screened

125   (Chow *et al.* 2016; Palu *et al.* 2019). These results reinforce the idea that different causative

126   genes and mutations will interact with different pathways over the course of disease. It also

127   highlights the importance of exploring multiple disease models in something so diverse as

128   diabetes, and the utility of the DGRP in precisely distinguishing modifiers of a particular

129   genotype-phenotype combination.

130

131   In this study, we report the results of a natural variation screen in a model of *Sirt1* loss-of-

132   function. Loss of this gene in *Drosophila* has been shown to lead to progressive metabolic

133   dysfunction including obesity, hyperglycemia, and ultimately insulin resistance (Palu and

134   Thummel 2016). Our study design is specifically focused on the phenotype of hyperglycemia

135   when *Sirt1* expression is disrupted using RNAi in the adipose and liver-like fat body organ. We

136   observed substantial phenotypic variation across the DGRP for hyperglycemia associated with

137   loss of *Sirt1*. Using genome-wide association analysis, pathway enrichment, and the generation

138   of a physical interaction network, we identified a number of modifying pathways and processes,

139   several of which have known roles in central carbon metabolism, the immune response, and the

140   kind of neuronal signaling and communication expected to influence the neuroendocrine cells

141   responsible for insulin secretion in *Drosophila*. Finally, we confirmed that loss of several of the

142   top candidate modifier genes significantly alters glucose levels in the *Sirt1* RNAi model. Our

143   findings highlight exciting new areas of study for modifiers of *Sirt1* function, glucose

144   homeostasis, and insulin sensitivity.

145

146   **METHODS**

147   *Fly stocks and maintenance*

148   Flies were raised at room temperature on a diet based on the Bloomington Stock Center

149   standard medium with malt. Experimental crosses were maintained on a media containing 6%

150   yeast, 6% dextrose, 3% sucrose, and 1% agar, with 0.6% propionic acid and 0.1% p-Hydroxy-

151   benzoic acid methyl ester in 95% ethanol included as antifungal agents. Flies subjected to an

152   overnight fast were transferred to media containing only 1% agar in water. The *R4>Sirt1i* strain,

153   which serves as the model of hyperglycemia in this study, is derived from an *R4-GAL4* strain

154   (BDSC 33832) outcrossed to w^{1118} (Palu and Thummel 2016) and a *Sirt1* RNAi strain from the

155   Bloomington Stock Center (32481). 185 strains from the DGRP were used for the modifier

156   screen (Tables S1-S3), wherein virgin females carrying the *R4>Sirt1i* model were crossed to

157   males of the DGRP strains. Male F1 progeny carrying *R4>Sirt1i* were separated and aged for

158   one to two weeks. These flies were then either collected under ad libitum fed conditions or

159   fasted overnight and then collected. The following RNAi and control strains are from the

160   Bloomington Stock Center: *CG4168* RNAi (28636), *CG5888* RNAi (62175), *uif* RNAi (38354),

161   *CTPSyn* RNAi (31924), *smt3* RNAi (36125), *ilp5* RNAi (33683), *Vha55* RNAi (40884), *snRNP-*

162   *U1-70k* RNAi (33396), *CG10265* RNAi (43294), *CG15803* RNAi (51449), *Roe* RNAi (57836),

163   *CG34353* RNAi (58291), *CadN2* RNAi (27508), *Ace* RNAi (25958), *CG43897* (31560), *dsxc73A*

164   RNAi (56987), *bgm* RNAi (56979), *CG3407* RNAi (57762), control *attP40* (36304), and control

165   *attP2* (36303).

166

167   *Glucose Assay*

168   Samples of five flies each were collected at one or two weeks of age and washed in 1XPBS.

169   Samples were then either frozen in liquid nitrogen and stored long-term at -80C or immediately

170   homogenized in 100 uL 1X PBS. Frozen samples were kept frozen until immediately upon

171   addition of PBS and homogenization. After homogenization samples were subjected to heat

172   inactivation of enzymes at 70C for approximately 10 minutes. Glucose was measured undiluted

173   from the lysate using the Sigma HK Glucose Assay kit as described (Tennessen *et al.* 2014).

174

175   *Protein Assay*

176   Prior to heat inactivation, 10 uL of the fly lysate isolated for glucose measurement was saved

177   and kept on ice. Protein samples could then be stored long term at -80ºC. Samples were

178   centrifuged for up to 5 minutes at room temperature and protein measured from the supernatant

179   after a 1:10 dilution using the Sigma Protein Assay Reagent as described (Tennessen *et al.*

180   2014).

181

182   *Phenotypic analysis and genome-wide association*

183   For each DGRP line, glucose was measured from 3 samples of 5 flies each. The P-values for

184   association of genetic background and glucose concentration were calculated using one-way

185   ANOVA on R software taking into account all collected data points for each experiment.

186   Average glucose concentration was used for the genome-wide association (GWA). GWA was

187   performed as previously described (Chow *et al.* 2016; Palu *et al.* 2019). DGRP genotypes were

188   downloaded from the website, http://dgrp.gnets.ncsu.edu/. Non-biallelic sites were removed. A

189   total of 3,636,891 variants were included in the analysis. Mean eye glucose concentration for

190   555 samples representing 2775 DGRP/R4>Sirt1i F1 progeny were regressed on each SNP. To

191   account for cryptic relatedness (He *et al.* 2014; Huang *et al.* 2014), GEMMA (v. 0.94) (Zhou and

192   Stephens 2012) was used to both estimate a centered genetic relatedness matrix and perform

193   association tests using the following linear mixed model (LMM):

194   $$y = \alpha + x\beta + u + \epsilon$$

195   $$u \sim MVN_n(0, \lambda\tau^{-1} K)$$

196   $$\epsilon \sim MVN_n(0, \tau^{-1} I_n)$$

197   where, as described and adapted from Zhou and Stephens 2012, y is the n-vector of average

198   glucose concentration for the n lines, α is the intercept, x is the n-vector of marker genotypes, β

199   is the effect size of the marker. u is a n x n matrix of random effects with a multivariate normal

200   distribution (MVN_n) that depends on λ, the ratio between the two variance components, τ^{-1},

201   the variance of residuals errors, and where the covariance matrix is informed by K, the

202   calculated n x n marker-based relatedness matrix. K accounts for all pairwise non-random

203   sharing of genetic material among lines. ϵ, is a n-vector of residual errors, with a multivariate

204   normal distribution that depends on τ^{-1} and I_n, the identity matrix. Quantile-quantile (qq)

205   plots demonstrate an appropriate fit to the LMM at the positive end of the plot, but a greater

206   number of points than expected by chance with an insignificant p-value (Figure S1). Genes

207   were identified from SNP coordinates using the BDGP R54/dm3 genome build. A SNP was

208   assigned to a gene if it was +/- 1 kb from a gene body.

209

210   *RNAi Validation*

211   Virgin females from the *R4>Sirt1i* model were crossed to males carrying RNAi constructs

212   targeting candidate modifiers of those models, and the glucose levels of F1 male progeny

213   expressing both *Sirt1i* and the modifier RNAi construct specifically in the fat body were

214   measured as described above on 4-5 samples of 5 male flies each. Glucose concentrations

215   from RNAi-carrying strains are compared directly to genetically matched *attP40* or *attP2*

216   controls using a Dunnett's multiple comparisons test. Glucose measurements are normalized to

217   the appropriate genetically matched controls. Normalized controls from individual experiments

218   are compared in Figure S2. Standard deviation did not significantly vary between controls for

219   individual experiments.

220

221   *Bioinformatics Analysis*

222   Genetic polymorphisms were associated with candidate genes within 1 kb of the polymorphism.

223   Information about candidate genes and their human orthologues was gathered from a number

224   of databases including Flymine, Flybase, OMIM, and NCBI. Physical interaction maps were

225   generated using the GeneMANIA plugin on Cytoscape (version 3.8.2) (Shannon *et al.* 2003;

226   Montojo *et al.* 2010). GSEA was run to generate a rank-list of genes based on their enrichment

227   for significantly associated polymorphisms. For GSEA analysis, polymorphisms within 1kb of

228   more than 1 gene were assigned to one gene based on a priority list of exon, UTR, intron, and

229   upstream or downstream. Genes were assigned to GO categories, and calculation of

230   enrichment score was performed as described (Subramanian *et al.* 2005). Categories with ES

231   scores > 0 (enriched for associated genes with low p-values), gene number > 3, and p-values

232   <0.05 were included in the final output.

233

234   **RESULTS**

235   *Glucose levels in R4>Sirt1i flies vary with genetic background in a consistent pattern across*

236   *multiple conditions*

237   Loss of *Sirt1* expression leads to progressive hyperglycemia, obesity, and insulin resistance. To

238   model the hyperglycemia that is commonly associated with diabetes, we reduced the

239   expression of the deacetylase *Sirt1* specifically in the fat body of *Drosophila melanogaster*.

240   RNAi targeting *Sirt1* specifically in the fat body reproduces the hyperglycemia phenotype, with

241   an approximately 50-60% increase in whole fly glucose levels (P = 0.02, Figure S3) (Palu and

242   Thummel 2016). The fat body in *Drosophila* performs functions normally undertaken by the

243   adipose and liver tissues in humans (Géminard *et al.* 2009; DiAngelo and Birnbaum 2009;

244   Arrese and Soulages 2010). While there are likely roles for *Sirt1* in other metabolic tissues, its

245   function in the fat body clearly contributes to the maintenance of glucose homeostasis and

246   insulin sensitivity over time (Palu and Thummel 2016). Modifiers of insulin signaling or glucose

247   metabolism could alter the degree of hyperglycemia in this model.

248

249   The degree of hyperglycemia is determined by a biochemical assay that measures the

250   concentration of glucose in a whole-fly lysate (Tennessen *et al.* 2014). This is a quantitative

251   assay where higher concentrations of glucose correlate with more severe hyperglycemia, and

252   lower concentrations of glucose correlate with milder disease, or potentially hypoglycemia.

253   Glucose was measured specifically in males, as adult female *Drosophila* devote much of their

254   physiological output to egg production (Millington and Rideout 2018). Previous studies have

255   demonstrated that adult males provide a consistent model for metabolic homeostasis in the fly

256   (Sieber and Thummel 2009; Tennessen *et al.* 2014; Palu and Thummel 2016; Barry and

257   Thummel 2016; Beebe *et al.* 2020).

258

259   Loss of *Sirt1* is induced using the *GAL4/UAS* system, where *R4-GAL4* drives expression of

260   *UAS-Sirt1* RNAi (Figure S4A). *R4-GAL4* is strongly expressed primarily in the fat body of fly,

261   starting in early development and continuing through adulthood (Lee and Park 2004). The line

262   containing this model (*R4>Sirt1i*) serves as the donor strain that was crossed to each DGRP

263   strain. Females from the donor strain were crossed with males of each of 185 DGRP strains to

264   generate F1 progeny lacking *Sirt1* expression in the fat body. The progeny received 50% of their

265   genome from the maternal donor strain and 50% from the paternal DGRP strain (Figure S4B).

266   Therefore, we are measuring the dominant effect of the DGRP background on the *Sirt1* RNAi

267   hyperglycemia phenotype. This experimental design is similar to a model of *NGLY1* deficiency

268   using RNAi that was also crossed to the DGRP (Talsness *et al.* 2020).

269

270   In the prior study characterizing the impact of the loss of function of *Sirt1* on metabolic

271   homeostasis, the dysfunction observed was progressive in nature. While larvae and young

272   adults are immediately obese, hyperglycemia and insulin resistance set in and become worse

273   with increasing age (Reis *et al.* 2010; Palu and Thummel 2016). To ensure an appropriate set of

274   conditions with respect to diet and age, we performed a preliminary analysis on 37 DGRP

275   strains at one or two weeks of age, and under fasted or ad libitum fed conditions (Table S1).

276   These time points correspond to conditions in the original study where differences in the

277   metabolic state of the flies corresponded to differences in glycemia (Palu and Thummel 2016).

278   We wished to select a time point at which hyperglycemia was detectable, but also differed

279   enough between strains to allow us to identify genetic variation associated with that

280   heterogeneity.

281

282   Three samples were collected for glucose measurements in each strain and condition. Glucose

283   levels vary across genetic background for each of the conditions being tested (Figure 1A-D).

284   Average glucose for each strain is significantly correlated between one and two week fasted

285   flies (R = 0.53, P = 4E-03), between one-week-old fed and fasted flies (R = 0.45, P = 0.020),

286   and between one-week-old fed and two-week-old fasted flies (R = 0.62, P = 2E-04) (Figure

287   S5A-C). This supports glucose concentration as a consistent quantitative measurement.

288   Interestingly, evidence for correlation with two-week-old flies fed ad libitum is not as strong.

289   While a significant correlation is still detected with one-week-old fasted flies (R = 0.43, P =

290   0.014), the correlation is not significant with two-week-old fasted flies (R = 0.25, P = 0.219) and

291   one-week-old flies fed ad libitum (R = 0.34, P = 0.063) (Figure S5D-F). By two weeks of age,

292   *Sirt1* loss-of-function flies are beginning to experience more severe symptoms of disease, and

293   we expect to see variability in symptoms and behavior in response to those symptoms. Fed flies

294   at two weeks may have more variable glucose because feeding behavior is a big contributor to

295   glucose levels in flies that have not been subjected to a fast.

296

297   To identify the conditions under which the impact of genetic background was the strongest, we

298   performed a one-way ANOVA test that included all data points collected. We found that while

299   there is a significant association between glucose levels and genetic background under all

300   conditions (p<0.05), this effect is most pronounced in the one-week-old flies fed ad libitum (P =

301   1.87E-5) and in the two-week-old fasted flies (P = 1.95E-5) (Figure 1A,D). Because fasting

302   reduces possible intra-strain variation caused by food in the gut, two weeks fasted was selected

303   for the full screen.

304

305   We examined protein concentrations in 90 samples from the first 30 strains collected at 2 weeks

306   fasted to ensure that any variation we observe in glucose is not due to differences in body size.

307   Protein levels do not significantly vary across the DGRP (P = 0.63, Figure S6A), nor do protein

308   levels correlate with glucose levels in individual samples (R = 0.04, P = 0.6577, Figure S6B).

309   We conclude that the variation we observe in fasting glucose levels are due to differences in

310   circulating glucose, and not to differences in body size.

311

312 *Genome-wide association analysis identifies candidate modifiers of Sirt1i-associated*

313 *hyperglycemia*

314 Using the conditions determined in the preliminary screen, we proceeded to cross the donor

315 strain with the remaining 149 DGRP strains (Figure 2, Tables S2,S3). We found a significant

316 effect of genetic background on glycemia in the R4>Sirt1i flies (P < 2E-16) using one-way

317 ANOVA including all data points for each strain (N = 555). Individual glucose measurements

318 ranged from 0.306 µg/fly to 3.416 µg/fly (Table S2), while average concentrations ranged from

319 0.395 µg/fly (RAL 801) to 2.438 µg/fly (RAL 357) (Figure 2, Table S3).

320

321 To identify genetic polymorphisms that may be responsible for this observed variation in

322 glycemia, we performed a genome-wide association analysis. Average glucose level for each

323 strain was used as a quantitative phenotype to test for association with polymorphisms in the

324 DGRP. A total of 3,636,891 variants were tested for the *R4>Sirt1i* model across 186 lines. This

325 analysis as a result is insufficiently powered for candidates to remain statistically significant after

326 multiple testing corrections. Instead, the focus is on identification of candidate modifiers and

327 pathways that can be validated through further study and that will provide the basis for future

328 projects. This approach has been quite successful in previous studies (Chow *et al.* 2013, 2015,

329 2016; Palu and Chow 2018; Lavoy *et al.* 2018; Palu *et al.* 2019, 2020; Talsness *et al.* 2020).

330

331 Because the analyzed F1 hybrids in this case were male and inherited their X chromosome from

332 the donor strain and not the DGRP strain, we do not include any X-linked variants in the

333 resulting candidate modifiers. Using an arbitrary cut-off of $P < 10^{-4}$, we identified 237

334 polymorphisms on the second and third chromosomes (Table S4). Of these 237, 62 were not

335 considered further as they were not within +/- 1 kb of a candidate gene. The remaining 175

336 polymorphisms are associated with a total of 161 candidate genes (Table S5). 100 of these

337 polymorphisms are intronic, 29 are exonic with 6 producing non-synonymous changes to the

338 peptide and one a start-gain, 10 are located in the 5' or 3' untranslated regions, and 36 are

339 within 1 kb up or downstream of the candidate gene (Table S4). Of note in this analysis is that

340 the results were not filtered for allele frequency > 0.05. This was a concerted choice; several of

341 the most interesting candidates, including *CG5888* and *ilp5*, would otherwise have been left out

342 of the analysis. The number of total variants analyzed drops from 237 to 90, and the number of

343 candidate genes associated at $P < 10^{-4}$ drops from 161 to 75. While this, along with the use of a

344 low stringency p-value cut-off, increases the probability of false positives, it likewise increases

345 our power when performing pathway enrichment. Validation of candidate genes with low minor

346 allele frequencies in later studies will distinguish true positives from false positives.

347

348 One concern with using an RNAi model to reduce *Sirt1* expression is that the modifiers

349 identified might be specific RNAi efficacy, rather than hyperglycemia. The modifiers could be

350 altering the degree and efficiency of *Sirt1* knockdown, so that hyperglycemia is actually

351 correlating with the amount of *Sirt1* expression that is achieved. If this were the case, we would

352 expect to see the top candidate modifiers associated with RNAi machinery or the efficiency of

353 the GAL4/UAS system. This does not appear to be the case, either from a single-gene function

354 perspective or when looking at enriched gene categories (Tables S5 and S6). Furthermore, the

355 GAL4/UAS system is commonly used to model disease in the DGRP, and the candidates

356 identified have always been unique to the disease and, at times, even the specific model in

357 question (He *et al.* 2014; Chow *et al.* 2016; Lavoy *et al.* 2018; Palu *et al.* 2019; Talsness *et al.*

358 2020). All of this suggests that the candidate genes identified through this screen are modifying

359 *Sirt1*-associated hyperglycemia directly rather than altering the degree of *Sirt1* knockdown.

360

361 *Candidate modifiers of Sirt1 are involved in basic metabolic processes, the immune response,*

362 *and the regulation of neuronal communication*

363   Because loss of *Sirt1* in the fat body alters glucose metabolism and insulin sensitivity in the

364   organism, we expected modifiers of hyperglycemia to impact pathways linked to central carbon

365   metabolism as well as external processes that influence secretion and signaling of hormones

366   such as insulin. To determine if this is the case, we examined the individual functions of the top

367   GWA candidates and looked for pathways and processes that are enriched in this list. While we

368   attempted first to do this through Gene Ontology analysis of our top candidates, we found no

369   significantly enriched terms. We therefore utilized individual known physical interactions and GO

370   term enrichment through GSEA to highlight likely candidate pathways.

371

372   **Analysis of Candidate Modifiers:** We expected our top candidates to include genes that

373   function in pathways or processes related to *Sirt1* regulation or activity. Among the most

374   interesting candidates are those involved in NAD metabolism. We identified two genes whose

375   products are part of the NADH dehydrogenase component of Complex I in the electron transport

376   chain (*NDUFS3* and *ND-PDSW*) (FlyBase Curators 2008; Gaudet *et al.* 2011). There are also

377   two NADP kinases, enzymes involved in the generation of NADP from NAD (*CG33156* and

378   *CG6145*) (Gaudet *et al.* 2011). *DUOX*, an NADPH oxidase, passes electrons from NADPH to

379   oxygen, generating hydrogen peroxide and altering the redox balance of the cell (Gaudet *et al.*

380   2011; Anh *et al.* 2011). As Sirt1 utilizes NAD as a cofactor during its enzymatic reaction, altering

381   the balance of NAD in the cell through differential regulation of these enzymes could further

382   impact the activity of other pathways that require NAD as an electron carrier, or exacerbate the

383   phenotypes associated with *Sirt1* loss-of function (Nogueiras *et al.* 2012). We also identified two

384   genes that have previously been implicated in the regulation and/or extension of lifespan: *sugb*

385   and *CG42663* (Landis *et al.* 2003; Paik *et al.* 2012). While the role of *Sirt1* in lifespan extension

386   is still contested, the identification of other genes implicated in this process suggests shared

387   functions or pathways.

388

389   Genes involved in central glucose metabolism as well as insulin signaling are also candidate

390   modifiers. MFS5 acts as a transporter of both glucose and trehalose for the uptake of these

391   sugars from circulation (McMullen *et al.* 2021). Glucose-6-phosphatase (*G6P*) is the last rate-

392   limiting step in both gluconeogenesis and glycogenolysis, which are used to generate glucose

393   for release into the body during fasting (Gaudet *et al.* 2011; Lizák *et al.* 2019). These two genes

394   directly regulate circulating glucose levels. Candidates involved in other metabolic pathways

395   include *CTPSyn*, which encodes the rate limiting step in cytidine synthesis, the very long chain

396   fatty acid ligase *bgm*, the mannosidase *Edem2*, and the oxoglutarate dehydrogenase complex

397   subunit *CG33791* (Kang and Ryoo 2009; Gaudet *et al.* 2011; Jang *et al.* 2015; Sivachenko *et al.*

398   2016; Zhou *et al.* 2019). Partially responsible for regulating general metabolic flux through these

399   various pathways is insulin. Interestingly, a top candidate is *ilp5*, one of several insulin-like

400   peptides expressed in the insulin-producing cells (IPCs) in the *Drosophila* brain (Géminard *et al.*

401   2009). Our analysis also identified *IA-2*, a phosphatase involved in ilp secretion, *CG4168*, an

402   uncharacterized gene whose closest human orthologue *IGFALS* encodes a protein that binds to

403   and stabilizes IGF proteins in circulation, and *wrd*, a subunit in the protein phosphatase PP2A

404   that negatively regulates insulin and TOR signaling (Boisclair *et al.* 1996; Kim *et al.* 2008; Hahn

405   *et al.* 2010).

406

407   Other potential modifiers of insulin stability and signaling in circulation are *dally*, *cow*, and *Hs3st-*

408   *A*. Both *dally* and *cow* encode heparin sulfate proteoglycans, while *Hs3st-A* encodes an O-

409   sulfotransferase that acts on these proteoglycans (Filmus and Selleck 2001; Gaudet *et al.* 2011;

410   Chang and Sun 2014). Previous work has demonstrated an impact of the enzyme heparanase,

411   which cleaves heparan sulfate, on diabetic autoimmunity and complications such as

412   nephropathy (Rabelink *et al.* 2017). While this is more peripheral to the central insulin signaling

413   pathway in *Drosophila*, it highlights the utility of such factors in altering disease processes in

414   subtle ways.

415

416   Another interesting group of candidates are those associated with neuronal development and

417   function. Several members of the defective proboscis extension response (*dpr*) family were

418   represented in our list (*dpr2*, *dpr6*, and *dpr13*) along with the dpr-interacting protein *DIP-eta*.

419   The *dpr* gene family is collectively associated with synapse organization and function, as are the

420   candidate genes *fife*, *CG32373*, and *atilla* (FlyBase Curators *et al.* 2004; Kurusu *et al.* 2008;

421   Carrillo *et al.* 2015; Bruckner *et al.* 2017). We also noted candidates involved in neuropeptide

422   signaling (*rk* and *RYa-R*), voltage-gated potassium channels and their regulation (*CG5888* and

423   *CG1688*), and axon guidance (*tutl*, *CadN2*, *CG34353*, and *sbb*) (Rao *et al.* 2000; Luo *et al.*

424   2005; Prakash *et al.* 2005; Al-Anzi and Wyman 2009; Ida *et al.* 2011; Gaudet *et al.* 2011). The

425   IPCs in *Drosophila* are actually neuroendocrine cells located in the brain, as are the AKH-

426   producing cells responsible for secreting the glucagon-like hormone AKH (Géminard *et al.*

427   2006). The secretion of insulin is therefore dependent upon the correct development,

428   connection, and signaling of neuronal cells.

429

430   The immune response is another generally enriched category of modifier genes. Several

431   members of the nimrod family of immunoglobulins (*NimB2*, *NimC1*, and *NimC3*) were identified

432   by GWA. All are implicated in the innate immune response, with *NimC1* and *NimC3* in particular

433   having roles in phagocytosis (Somogyi *et al.* 2010). In response to insecticides, *LRR* regulates

434   the immune response through NF-kappaB, whose activation is an early protective event in the

435   progression and pathology of diabetes (Prisco *et al.* 2013; Irvin *et al.* 2018). Two lysozyme

436   enzymes with links to bacterial defense (*LysX* and *CG7798*) highlight the role of oxidative stress

437   and redox homeostasis in the innate immune response (FlyBase Curators 2008). As Sirt1 has

438   roles in regulating the response to oxidative stress, we looked for other genes with similar

439   functions (Brunet *et al.* 2004). As described above, *DUOX* plays a part in regulating redox

440   homeostasis through the production of hydrogen peroxide (Anh *et al.* 2011). *CG42331* encodes

441 a peroxidase that appears to be strongly enriched in the pupal fat body, and *cyp28a5* encodes

442 an oxidoreductase that, similar to LRR, is involved in the response to insecticides (FlyBase

443 Curators *et al.* 2004; Graveley *et al.* 2011; Gaudet *et al.* 2011). It is now believed that Type I

444 and Type II diabetics both suffer at least to some degree from autoimmunity (Candia *et al.*

445 2019). Exploring the direct and indirect connections of *Sirt1* to the immune response and

446 oxidative stress directly is an interesting avenue for future direction.

447

448 **Physical Interaction Network:** We generated a network of physical interactions among the 161

449 candidate genes identified above. These were identified and visualized using Cytoscape

450 software with the GeneMania plugin (Shannon *et al.* 2003; Montojo *et al.* 2010). The products of

451 37/161 candidate genes were found to physically interact with at least one other candidate gene

452 product with no more than one bridging node represented by a non-candidate gene (Figure 3A).

453 This high degree of interaction suggests that the modifiers identified in this screen are indeed

454 functioning through shared processes.

455

456 Focusing then on the 37 genes involved in physical interactions, we identified several broad

457 functional categories that could influence glucose homeostasis in the fly. The most obvious

458 category are enzymes that catalyze steps in basic metabolic pathways (N = 7). This includes

459 the NAD kinases (*CG6145* and *CG33156*) and one NADH dehydrogenase (*ND-PDSW*)

460 discussed above (Gaudet *et al.* 2011). Other metabolic candidate modifiers include *MFS3* and

461 *CTPsyn*, the rate limiting enzyme in the production of the nucleotide Cytidine triphosphate (Zhou

462 *et al.* 2019). Both of these enzymes function in pathways critically dependent upon or feeding

463 into central carbon metabolism, and their inclusion as candidate modifiers of hyperglycemia

464 supports a role for those secondary metabolic pathways as a sink for increased circulating

465 glucose. *Mtmr6* encodes a phosphatidylinositol phosphatase, a key enzyme in several signaling

466 pathways, including insulin signaling (Gaudet *et al.* 2011). Also interesting is the gene *LRP1*,

467   which is orthologous to human LDL receptor related protein 1. In additional to its role in lipid

468   homeostasis, *LRP1* has also been implicated in Alzheimer's disease, for which metabolic

469   disease and obesity are risk factors (Kang *et al.* 2000; Anstey *et al.* 2011).

470

471   Curiously, several of the genes highlighted in this analysis also happen to localize specifically to

472   the mitochondria (N = 4). *Roe1* and *porin* are both transporters involved in the import of

473   molecules into the mitochondria (Komarov *et al.* 2004; Jana Alonso *et al.* 2005; FlyBase

474   Curators 2008; Gaudet *et al.* 2011). The NADH dehydrogenases *ND-PDSW* and *NDUFS3* both

475   function in the mitochondria as well as part of Complex I in the electron transport chain

476   (Jana Alonso *et al.* 2005). Closer examination of the top GWA candidates reveals additional

477   mitochondrial localization candidates including the amino acyl tRNA synthetase *GlyRS*, the

478   membrane bound regulator of protein kinase A (*pkaap*) and the translation elongation factor

479   *mEFTu1* (Gaudet *et al.* 2011; Lu *et al.* 2016). In adult metabolic homeostasis, central carbon

480   metabolism is generally used to fuel the electron transport chain in the mitochondria and

481   generate ATP for the cell (Barry and Thummel 2016). Altering the activity of this essential

482   downstream pathway could have a clear impact on glucose utilization and disease progression

483   in diabetes.

484

485   Similar to our examination of top candidates, our physical interaction map highlighted the

486   immune response (*NimC1*, *NimC3*, *NimB2*, and *LRR*) and neuronal function. *Tutl*, *dpr2*, and

487   *DIP-eta,* and *wb* are all involved in synapse organization and axon guidance, while *Pax* and

488   *rhea* are involved in focal adhesion (Delon and Brown 2009). The identification of genes

489   important for cellular communication suggests that some of the modifiers identified in this study

490   have roles in tissues other than the fat body, such as the IPC and APC neurons. This is an

491   important avenue of future exploration.

492

493   **Gene Set Enrichment Analysis (GSEA):** In the second approach, we performed GSEA

494   analysis to identify gene ontology terms for which associated variants are enriched. Unlike

495   traditional GO analysis, which relies upon a set of genes based on a P-value cutoff, GSEA

496   examines the entire gene set (Dyer *et al.* 2008). For each defined GO category, GSEA

497   determines whether the members of that category are randomly distributed throughout the

498   ranked gene list provided or if they are enriched for the lower p-values found at the top of that

499   list. GO categories enriched at the top of the list describe important functions of the gene set.

500   GSEA identified 52 significantly associated gene sets (≥ 3 genes) with positive enrichment

501   scores at a p-value of <0.05 (Table S6, Figure 3B). The top two gene sets implicate neuronal

502   function and communication in the *Sirt1i*-associated hyperglycemia phenotype: calcium-

503   activated potassium channel activity (GO:0015269, P = 1.1E-3) and maintenance of presynaptic

504   active zone structure (GO:0048790, P = 1.2E-3). Similar categories can be found through the

505   list of significantly associated gene sets, including dendrite morphogenesis (GO:0048813, P =

506   0.049), which represents the largest group of genes at N = 119 and contains two of the top

507   GWA candidates (*slit* and *fruitless*). Coupled with the neuronal genes identified in our physical

508   interaction network, this suggests that function in the neuroendocrine cells could play a big role

509   in glucose homeostasis in the fat body.

510

511   Also enriched are taste receptor activity (GO:0008527, P = 0.013) and sensory reception of

512   taste (GO:0050909, P = 0.018). These categories highlight a yet unconsidered factor that must

513   be taken into account with metabolic phenotypes: that of feeding and diet. While all flies were

514   collected under identical conditions and were maintained on the same diet, it is nonetheless

515   possible that some may simply be eating more due to differences in the sensing of satiation or

516   to differences in perception of taste. These differences in perception and consumption can have

517   detectable impacts on metabolic phenotypes (May *et al.* 2019).

518

519   As expected, we also see evidence of general metabolic processes. Some, like alpha,alpha-

520   trehalase activity (GO:0004555, P = 0.043) and phosphatidylinositol transporter activity

521   (GO:0008526, P = 0.013) have direct links to glucose metabolism and insulin signaling. Others,

522   such as oxysterol binding (GO:0008142, P = 0.026), glutamate biosynthetic process

523   (GO:0006537, P = 0.043), and isoprenoid biosynthetic process (GO:0008299, P = 0.048)

524   function more peripherally to carbon metabolism and are likely influencing hyperglycemia by

525   their general contribution to physiological homeostasis.

526

527   Another interesting group of GO categories highlighted by GSEA are RNA processing functions.

528   rRNA (uridine-2'-O-)-methyltransferase activity (GO:0008650, P = 2.4E-3) is the fourth most

529   associated category as ranked by p-value, and others such as snoRNA binding (GO:0030515, P

530   = 0.014) reiterating this function. The presence of RNA processing categories is of particular

531   interest because three of the top candidate genes by GWA are splicing factors (*bru1*, *fand*, and

532   *snRNP-U1-70k*) (Park *et al.* 2004; Oas *et al.* 2014; Spletter *et al.* 2015). While it is unclear how

533   rRNA or mRNA processing may directly or indirectly influence glucose homeostasis in

534   particular, the identification of this process through several different methods of analysis is

535   striking and worth further exploration.

536

537   *Functional analysis of candidate modifier genes*

538   To confirm the roles of our candidate genes in regulating glucose homeostasis, we elected to

539   test the impact of loss of modifier expression for 16 of the most significant candidates for which

540   we were able to obtain transgenic RNAi lines (Table 1). We crossed the RNAi strains targeting

541   each of these modifiers into the *R4>Sirt1i* line, aged the resulting progeny for 2-3 weeks, and

542   measured glucose in fasted males. We also measured protein levels as a control. Knockdown of

543   modifier genes did not significantly alter protein levels as compared to a genetically matched

544   control (Figure S7). Knockdown of the genes *CG4168*, *CG5888*, and *uif* resulted in suppression

545   of the hyperglycemia phenotype, with a significant decrease in glucose content per fly compared

546   to controls expressing *R4>Sirt1i* (Figure 4). These results demonstrate that many of the top

547   GWA candidate modifiers are capable of modifying the hyperglycemia phenotypes associated

548   with the *R4>Sirt1i* model of diabetes.

549

550   **DISCUSSION**

551   Identifying and characterizing the genetic factors influencing the severity of diabetes is critical to

552   early diagnosis. Prevention is still the best strategy available, and providing patients at high risk

553   for complications with knowledge of that risk could prevent the worst symptoms from

554   manifesting. It could even enable intervention before the progression of disease is irreversible.

555

556   In this study, we identified and analyzed a number of candidate modifiers of hyperglycemia in a

557   previously characterized model of diabetes, *Sirt1* loss-of-function. We used the DGRP as an

558   unbiased source of natural genetic variation for this screen. This is the first time a genetic model

559   of metabolic dysfunction has been put to this use, as previous screens have either focused on

560   dietary stress as a source of metabolic disease or on the impact of genotype on metabolic

561   parameters under non-stressed conditions (Mackay *et al.* 2012; Ivanov *et al.* 2015; Nelson *et al.*

562   2016; Jehrke *et al.* 2018; Everman *et al.* 2019). We observed very little overlap in modifier

563   candidates between our observations and these studies. This is consistent with previous work

564   demonstrating that even when the observed phenotypes are similar or nearly identical, the

565   overlap in modifiers is often small in different models of disease (Palu *et al.* 2019). One

566   exception is a screen for the response to starvation resistance performed by Everman *et al.* in

567   2018. They identified *CG15803*, a transporter of unknown function that was also identified in our

568   studies (Everman and Morgan 2018). While our preliminary analysis suggests that this gene

569   does not function in the fat body, it is possible that it could have a role in another physiologically

570   relevant tissue such as the IPCs or APCs. Indeed, *CG15803* appears to be most highly

571   expressed in the head and CNS (Graveley *et al.* 2011). This is an interesting avenue of future

572   exploration.

573

574   We did observe overlap in general gene categories with previous studies, even when direct

575   overlaps were few. This was found to be true for modifiers of neuronal function. In a broad

576   exploration of genetic variation in the nutrient response that looked at triglycerides, starvation

577   resistance, mass, and glucose, *NimB3* was identified as a candidate modifier (Nelson *et al.*

578   2016). While *NimB3* was not identified in this screen, we did find *NimB2*, *NimC1*, and *NimC3*.

579   *Fife*, which also has roles in synapse organization, was identified in this study and one for

580   starvation resistance (Mackay *et al.* 2012). As mentioned above, both the IPCs and APCs are

581   neuroendocrine cells found in or near the brain (Géminard *et al.* 2006). Maintenance of neuronal

582   function would be critical to hormonal balance as a result. Furthermore, it is broadly

583   acknowledged that metabolic homeostasis is also dependent upon feeding rate, over which the

584   central nervous system has some sway (Owusu-Ansah and Perrimon 2014). The identification

585   of neuronal genes in each analysis suggests that regulation of particular neuronal pathways and

586   cells is critical to the maintenance of physiological homeostasis.

587

588   Given the prevalence of neuronal and sensory perception genes in the analysis, a concern

589   could be raised for the role feeding rate could be playing in the variation of glucose across the

590   DGRP. To assess this, we compared glucose with male feeding rate in a previous analysis

591   (Table S3) (Garlapow *et al.* 2015). We saw no correlation whatsoever, indicating that while

592   nutrient sensing may play a role in the response to Sirt1i-induced hyperglycemia, it is not the

593   driving factor in the variation observed in this screen (Figure S8).

594

595   Another interesting category highlighted through several analysis methods is the innate immune

596   response. While it has long been known that Type I diabetes is an autoimmune disorder, it has

597   recently been acknowledged that Type II diabetics also display symptoms of autoimmunity

598   (Candia *et al.* 2019). Furthermore, insulin resistance has frequently been associated with

599   inflammation, and the presence of macrophages in the adipose tissue is a hallmark of obesity

600   and diabetes (Wu and Ballantyne 2020). Modifiers associated with innate immunity serve

601   therefore as validation to the study as a whole, and examination of these genes and their

602   function in the context of the *Sirt1* loss-of-function model will be an intriguing focus of future

603   research.

604

605   An important component of this study is the validation of top candidate modifiers using RNAi-

606   mediated knockdown of gene expression. We obtained strains expression transgenic RNAi

607   constructs targeting 16 of the most significant candidates (Table 1). We found that reduced

608   expression of three candidates specifically in the fat body resulted in significant suppression of

609   hyperglycemia: *CG4168*, *CG5888*, and *uif* (Figure 4). We also noted a consistent, though not

610   significant, decrease in glucose for two independent RNAi constructs targeting *CTPSyn*,

611   suggesting that this gene warrants further study (Figure 4, data not shown). The remainder of

612   the genes had no significant or consistent impact on hyperglycemia in the model of *Sirt1* loss-of-

613   function (Figure 4). There were no enhancing modifiers: loss of modifier expression did not lead

614   to increased glucose levels for any of the tested genes. This could be because hyperglycemia is

615   already quite strong in the *Sirt1* loss-of-function model, or because we simply did not hit on any

616   enhancing modifiers. Of greater concern is the lack of any response for 13 of the 16 tested

617   candidates. One explanation may be found in the large number of known neuronal genes

618   identified in this analysis. This modifier RNAi screen specifically focused on the expression of

619   the RNAi against the candidate genes in the fat body, where expression of *Sirt1* is also reduced.

620   If, however, the function of a modifier gene is primarily concentrated in the IPCs, as with *ilp5*,

621   reducing its expression in the fat body would have little effect on the disease phenotypes in

622   question. We will examine the role of modifier genes not only in the fat body but in the IPCs,

623   APCs, and other physiologically relevant tissues in future work.

624

625   Of immediate interest is of course the mechanism of action for the three suppressor genes that

626   were confirmed by RNAi in the fat body. Of these, *CG5888* is also the top GWA candidate (P =

627   2.80E-07). While largely uncharacterized, *CG5888* has been identified as a component or

628   activator of voltage-gated potassium channels by sequence homology (Gaudet *et al.* 2011).

629   Intriguingly, it has also been implicated JNK signaling by a previous RNAi screen (Bond and

630   Foley 2009). JNK signaling is commonly activated by cellular stress and can activate apoptosis.

631   It also has important roles in the signaling pathways commonly used by the immune system

632   (Bond and Foley 2009; Shlevkov and Morata 2012). A potential role for *CG5888* in immune

633   pathways has yet to be explored and could be an exciting area of further discovery.

634

635   *Uninflatable* (*uif*) encodes a single pass transmembrane protein found on the apical membrane

636   of epithelial cells and has been found to enable Notch signaling (Loubéry *et al.* 2014). It has

637   also been found to exacerbate disease in a *Drosophila* model of muscular dystrophy

638   (Kucherenko *et al.* 2011), and its closest human orthologue ELAPOR1 is a regulator of

639   apoptosis and autophagy (Deng *et al.* 2010). Both of these processes are commonly disrupted

640   through inappropriate activation in metabolic disease, and might provide some explanation for

641   the impact of *uif* on *Sirt1i*-associated phenotypes (Bugliani *et al.* 2019).

642

643   Perhaps the most intriguing finding is *CG4168* as the modifier with the strongest impact on

644   *Sirt1i*-associated hyperglycemia. The protein encoded by *CG4168* is of unknown function, but

645   its closest human orthologue (*IGFALS*) encodes a serum protein that binds to insulin-like growth

646   factors (IGF) in circulation (Boisclair *et al.* 1996). In mammals, association with IGFALS

647   increases the half-life of insulin-like growth factors in the serum as well as their retention in

648 circulation. While studies of IGFALS in mammals has not shown a role for it in regulating insulin

649 signaling, the *Drosophila* ilp peptides are used for both IGF and insulin signaling activation

650 (Géminard *et al.* 2006). It is possible that secretion of the factor encoded by *CG4168* from the

651 fat body could increase ilp retention in circulation, whereas its loss could result in faster

652 clearance of ilps from circulation. Under conditions that promote insulin resistance, such as the

653 loss of *Sirt1*, it is possible that reduced ilp levels in the hemolymph could slow or prevent insulin

654 resistance and hyperglycemia. Further exploration of the mechanisms behind the action of

655 *CG4168* could reveal important insights into circulating insulin-binding factors and their role in

656 diabetes.

657

658 In conclusion, we have identified a number of pathways and processes involved in the degree of

659 hyperglycemia in a genetic model of diabetes. Examination of the candidate genes and

660 pathways described above in this model as well as other models of metabolic dysfunction will

661 shed new light on the mechanism by which insulin resistance and related complications disease

662 onset, progression, and severity. Furthermore, the candidates identified as suppressors could

663 serve as promising targets for therapeutics in diabetes and related metabolic disorders.

664

665   **DATA AVAILABILITY STATEMENT**

666 Strains and stocks are available upon request, as is code for GSEA. Genomic sequence for the

667 DGRP is available at http://dgrp.gnets.ncsu.edu/. Supplemental material is available at FigShare

668 (https://figshare.com/s/2b0b0237de0f94139a4f).

669

670   **ACKNOWLEDGEMENTS**

673   Summer Research Grant through the Purdue University-Fort Wayne Office of Sponsored

674   Projects to RASP as well as the Purdue University-Fort Wayne Department of Biology.

675

676   **REFERENCES**

677   Al-Anzi B., and R. J. Wyman, 2009 The Drosophila immunoglobulin gene turtle encodes

678   guidance molecules involved in axon pathfinding. Neural Dev. 2009 41 4: 1–15.

679   https://doi.org/10.1186/1749-8104-4-31

680   Anh N. T. T., M. Nishitani, S. Harada, M. Yamaguchi, and K. Kamei, 2011 Essential Role of

681   Duox in Stabilization of Drosophila Wing. J. Biol. Chem. 286: 33244–33251.

682   https://doi.org/10.1074/JBC.M111.263178

683   Anstey K. J., N. Cherbuin, M. Budge, and J. Young, 2011 Body mass index in midlife and late-

684   life as a risk factor for dementia: a meta-analysis of prospective studies. Obes. Rev. 12:

685   e426–e437. https://doi.org/10.1111/J.1467-789X.2010.00825.X

686   Arrese E. L., and J. L. Soulages, 2010 Insect Fat Body: Energy, Metabolism, and Regulation.

687   Annu. Rev. Entomol. 55: 207–225. https://doi.org/10.1146/annurev-ento-112408-085356

688   Barroso I., and M. I. McCarthy, 2019 The Genetic Basis of Metabolic Disease. Cell 177: 146–

689   161. https://doi.org/10.1016/j.cell.2019.02.024

690   Barry W. E., and C. S. Thummel, 2016 The Drosophila HNF4 nuclear receptor promotes

691   glucose-stimulated insulin secretion and mitochondrial function in adults. Elife 5.

692   https://doi.org/10.7554/ELIFE.11183

693   Beebe K., M. M. Robins, E. J. Hernandez, G. Lam, M. A. Horner, *et al.*, 2020 Drosophila

694   estrogen-related receptor directs a transcriptional switch that supports adult glycolysis and

695   lipogenesis. Genes Dev. 34: 701. https://doi.org/10.1101/GAD.335281.119

696   Biason-Lauber A., M. Böni-Schnetzler, B. P. Hubbard, K. Bouzakri, A. Brunner, *et al.*, 2013

697   Identification of a SIRT1 Mutation in a Family with Type 1 Diabetes. Cell Metab. 17: 448–

698   455. https://doi.org/10.1016/J.CMET.2013.02.001

699 Boisclair Y. R., D. Seto, S. Hsieh, K. R. Hurst, and G. T. Ooi, 1996 Organization and

700   chromosomal localization of the gene encoding the mouse acid labile subunit of the insulin-

701   like growth factor binding complex. Proc. Natl. Acad. Sci. 93: 10028–10033.

702   https://doi.org/10.1073/PNAS.93.19.10028

703 Bond D., and E. Foley, 2009 A quantitative RNAi screen for JNK modifiers identifies Pvr as a

704   novel regulator of Drosophila immune signaling. PLoS Pathog. 5.

705   https://doi.org/10.1371/JOURNAL.PPAT.1000655

706 Botden I. P. G., M. C. Zillikens, S. R. de Rooij, J. G. Langendonk, A. H. J. Danser, *et al.*, 2012

707   Variants in the SIRT1 Gene May Affect Diabetes Risk in Interaction With Prenatal

708   Exposure to Famine. Diabetes Care 35: 424–426. https://doi.org/10.2337/DC11-1203

709 Boutant M., and C. Cantó, 2014 SIRT1 metabolic actions: Integrating recent advances from

710   mouse models. Mol. Metab. 3: 5–18.

711 Bruckner J. J., H. Zhan, S. J. Gratz, M. Rao, F. Ukken, *et al.*, 2017 Fife organizes synaptic

712   vesicles and calcium channels for high-probability neurotransmitter release. J. Cell Biol.

713   216: 231–246. https://doi.org/10.1083/JCB.201601098

714 Brunet A., L. Sweeney, J. Sturgill, K. Chua, P. Greer, *et al.*, 2004 Stress-dependent regulation

715   of FOXO transcription factors by the SIRT1 deacetylase. Science 303: 2011–2015.

716   https://doi.org/10.1126/SCIENCE.1094637

717 Bugliani M., S. Mossuto, F. Grano, M. Suleiman, L. Marselli, *et al.*, 2019 Modulation of

718   Autophagy Influences the Function and Survival of Human Pancreatic Beta Cells Under

719   Endoplasmic Reticulum Stress Conditions and in Type 2 Diabetes. Front. Endocrinol.

720   (Lausanne). 10: 52. https://doi.org/10.3389/fendo.2019.00052

721 Cabrera A. P., R. N. Mankad, L. Marek, R. Das, S. Rangasamy, *et al.*, 2020 Genotypes and

722   Phenotypes: A Search for Influential Genes in Diabetic Retinopathy. Int. J. Mol. Sci. 2020,

723   Vol. 21, Page 2712 21: 2712. https://doi.org/10.3390/IJMS21082712

724 Candia P. de, F. Prattichizzo, S. Garavelli, V. De Rosa, M. Galgani, *et al.*, 2019 Type 2

725   Diabetes: How Much of an Autoimmune Disease? Front. Endocrinol. (Lausanne). 10: 451.

726   https://doi.org/10.3389/FENDO.2019.00451

727 Carrillo R. A., E. Özkan, K. P. Menon, S. Nagarkar-Jaiswal, P.-T. Lee, *et al.*, 2015 Control of

728   Synaptic Connectivity by a Network of Drosophila IgSF Cell Surface Proteins. Cell 163:

729   1770–1782. https://doi.org/10.1016/J.CELL.2015.11.022

730 CDC, 2020 National Diabetes Statistics Report 2020. Estimates of diabetes and its burden in

731   the United States.

732 Chang Y.-H., and Y. H. Sun, 2014 Carrier of Wingless (Cow), a Secreted Heparan Sulfate

733   Proteoglycan, Promotes Extracellular Transport of Wingless. PLoS One 9: e111573.

734   https://doi.org/10.1371/JOURNAL.PONE.0111573

735 Chow C. Y., M. F. Wolfner, and A. G. Clark, 2013 Using natural variation in Drosophila to

736   discover previously unknown endoplasmic reticulum stress genes. Proc Natl Acad Sci U S

737   A 110: 9013–9018. https://doi.org/10.1073/pnas.1307125110

738 Chow C. Y., F. W. Avila, A. G. Clark, and M. F. Wolfner, 2015 Induction of excessive

739   Endoplasmic reticulum stress in the Drosophila male accessory gland results in infertility.

740   PLoS One 10: 1–12. https://doi.org/10.1371/journal.pone.0119386

741 Chow C. Y., 2016 Bringing genetic background into focus. Nat. Rev. Genet. 17: 63–64.

742   https://doi.org/10.1038/nrg.2015.9

743 Chow C. Y., K. J. P. Kelsey, M. F. Wolfner, and A. G. Clark, 2016 Candidate genetic modifiers

744   of retinitis pigmentosa identified by exploiting natural variation in Drosophila. Hum. Mol.

745   Genet. 25: 651–659. https://doi.org/10.1093/HMG/DDV502

746 Chow C. Y., and L. T. Reiter, 2017 Etiology of Human Genetic Disease on the Fly. Trends

747   Genet. 33: 391–398. https://doi.org/10.1016/j.tig.2017.03.007

748 Delon I., and N. H. Brown, 2009 The integrin adhesion complex changes its composition and

749   function during morphogenesis of an epithelium. J. Cell Sci. 122: 4363–4374.

750   https://doi.org/10.1242/JCS.055996

751   Deng L., J. Feng, and R. R. Broaddus, 2010 The novel estrogen-induced gene EIG121

752   regulates autophagy and promotes cell survival under stress. Cell Death Dis. 1: e32.

753   https://doi.org/10.1038/CDDIS.2010.9

754   DiAngelo J. R., and M. J. Birnbaum, 2009 Regulation of Fat Cell Mass by Insulin in Drosophila

755   melanogaster. Mol. Cell. Biol. 29: 6341–6352. https://doi.org/10.1128/mcb.00675-09

756   Dyer M. D., T. M. Murali, and B. W. Sobral, 2008 The Landscape of Human Proteins Interacting

757   with Viruses and Other Pathogens. PLoS Pathog. 4: e32.

758   https://doi.org/10.1371/journal.ppat.0040032

759   Everman E. R., and T. J. Morgan, 2018 Antagonistic pleiotropy and mutation accumulation

760   contribute to age-related decline in stress response. Evolution (N. Y). 72: 303–317.

761   https://doi.org/10.1111/EVO.13408

762   Everman E. R., C. L. McNeil, J. L. Hackett, C. L. Bain, and S. J. Macdonald, 2019 Dissection of

763   Complex, Fitness-Related Traits in Multiple Drosophila Mapping Populations Offers Insight

764   into the Genetic Control of Stress Resistance. Genetics 211: 1449–1467.

765   https://doi.org/10.1534/genetics.119.301930

766   Filmus J., and S. B. Selleck, 2001 Glypicans: proteoglycans with a surprise. J. Clin. Invest. 108:

767   497–501. https://doi.org/10.1172/JCI13712

768   Flegal K., D. Kruszon-Moran, M. Carroll, C. Fryar, and C. Ogden, 2016 Trends in Obesity

769   Among Adults in the United States, 2005 to 2014. JAMA 315: 2284–2291.

770   https://doi.org/10.1001/JAMA.2016.6458

771   FlyBase Curators, Swiss-Prot Project Members, and InterPro Project Members, 2004 Gene

772   Ontology annotation in FlyBase through association of InterPro records with GO terms.

773   FlyBase Curators, 2008 Assigning Gene Ontology (GO) terms by sequence similarity in

774   FlyBase.

775   Garlapow M. E., W. Huang, M. T. Yarboro, K. R. Peterson, and T. F. C. Mackay, 2015

776   Quantitative Genetics of Food Intake in Drosophila melanogaster. PLoS One 10:

777   e0138129. https://doi.org/10.1371/JOURNAL.PONE.0138129

778 Gaudet P., M. S. Livstone, S. E. Lewis, and P. D. Thomas, 2011 Phylogenetic-based

779   propagation of functional annotations within the Gene Ontology consortium. Brief.

780   Bioinform. 12: 449–462. https://doi.org/10.1093/bib/bbr042

781 Géminard C., N. Arquier, S. Layalle, M. Bourouis, M. Slaidina, *et al.*, 2006 Control of

782   metabolism and growth through insulin-like peptides in Drosophila. Diabetes 55: S5–S8.

783   https://doi.org/10.2337/db06-S001

784 Géminard C., E. J. Rulifson, and P. Léopold, 2009 Remote Control of Insulin Secretion by Fat

785   Cells in Drosophila. Cell Metab. 10: 199–207. https://doi.org/10.1016/j.cmet.2009.08.002

786 Graveley B. R., G. May, A. N. Brooks, J. W. Carlson, L. Cherbas, *et al.*, 2011 The D.

787   melanogaster transcriptome: modENCODE RNA-Seq data for dissected tissues

788 Hahn K., M. Miranda, V. A. Francis, J. Vendrell, A. Zorzano, *et al.*, 2010 PP2A Regulatory

789   Subunit PP2A-B′ Counteracts S6K Phosphorylation. Cell Metab. 11: 438–444.

790   https://doi.org/10.1016/J.CMET.2010.03.015

791 He B. Z., M. Z. Ludwig, D. A. Dickerson, L. Barse, B. Arun, *et al.*, 2014 Effect of Genetic

792   Variation in a Drosophila Model of Diabetes-Associated Misfolded Human Proinsulin.

793   Genetics 196: 557. https://doi.org/10.1534/GENETICS.113.157800

794 Huang W., A. Massouras, Y. Inoue, J. Peiffer, M. Ràmia, *et al.*, 2014 Natural variation in

795   genome architecture among 205 Drosophila melanogaster Genetic Reference Panel lines.

796   Genome Res. 24: 1193–208. https://doi.org/10.1101/gr.171546.113

797 Ida T., T. Takahashi, H. Tominaga, T. Sato, K. Kume, *et al.*, 2011 Identification of the novel

798   bioactive peptides dRYamide-1 and dRYamide-2, ligands for a neuropeptide Y-like

799   receptor in Drosophila. Biochem. Biophys. Res. Commun. 410: 872–877.

800   https://doi.org/10.1016/J.BBRC.2011.06.081

801 Irvin A. E., G. Jhala, Y. Zhao, T. S. Blackwell, B. Krishnamurthy, *et al.*, 2018 NF-κB is weakly

802   activated in the NOD mouse model of type 1 diabetes. Sci. Reports 2018 81 8: 1–7.

803   https://doi.org/10.1038/s41598-018-22738-3

804 Ivanov D. K., V. Escott-Price, M. Ziehm, M. M. Magwire, T. F. C. Mackay, *et al.*, 2015 Longevity

805   GWAS using the drosophila genetic reference panel. Journals Gerontol. - Ser. A Biol. Sci.

806   Med. Sci. 70: 1470–1478. https://doi.org/10.1093/gerona/glv047

807 Ivy J., A. Klar, and J. Hicks, 1986 Cloning and characterization of four SIR genes of

808   Saccharomyces cerevisiae. Mol. Cell. Biol. 6: 688–702.

809   https://doi.org/10.1128/MCB.6.2.688-702.1986

810 Jana Alonso, Javier M. Rodriguez, and Luis Alberto Baena-López, and J. F. Santarén*, 2005

811   Characterization of the Drosophila melanogaster Mitochondrial Proteome. J. Proteome

812   Res. 4: 1636–1645. https://doi.org/10.1021/PR050130C

813 Jang B.-Y., H. D. Ryoo, J. Son, K.-C. Choi, D.-M. Shin, *et al.*, 2015 Role of Drosophila EDEMs

814   in the degradation of the alpha-1-antitrypsin Z variant. Int. J. Mol. Med. 35: 870–876.

815   https://doi.org/10.3892/IJMM.2015.2109

816 Jehrke L., F. A. Stewart, A. Droste, and M. Beller, 2018 The impact of genome variation and diet

817   on the metabolic phenotype and microbiome composition of Drosophila melanogaster. Sci.

818   Rep. 8. https://doi.org/10.1038/S41598-018-24542-5

819 Kang D. E., C. U. Pietrzik, L. Baum, N. Chevallier, D. E. Merriam, *et al.*, 2000 Modulation of

820   amyloid β-protein clearance and Alzheimer's disease susceptibility by the LDL receptor–

821   related protein pathway. J. Clin. Invest. 106: 1159–1166. https://doi.org/10.1172/JCI11013

822 Kang M.-J., and H. D. Ryoo, 2009 Suppression of retinal degeneration in Drosophila by

823   stimulation of ER-associated degradation. Proc. Natl. Acad. Sci. U. S. A. 106: 17043–8.

824   https://doi.org/10.1073/pnas.0905566106

825 Kim J., H. Bang, S. Ko, I. Jung, H. Hong, *et al.*, 2008 Drosophila ia2 modulates secretion of

826   insulin-like peptide. Comp. Biochem. Physiol. Part A Mol. Integr. Physiol. 151: 180–184.

827   https://doi.org/10.1016/J.CBPA.2008.06.020

828 Komarov A. G., B. H. Graham, W. J. Craigen, and M. Colombini, 2004 The Physiological

829   Properties of a Novel Family of VDAC-Like Proteins from Drosophila melanogaster.

830   Biophys. J. 86: 152–162. https://doi.org/10.1016/S0006-3495(04)74093-X

831 Kucherenko M. M., A. K. Marrone, V. M. Rishko, H. de F. Magliarelli, and H. R. Shcherbata,

832   2011 Stress and muscular dystrophy: A genetic screen for Dystroglycan and Dystrophin

833   interactors in Drosophila identifies cellular stress response components. Dev. Biol. 352:

834   228–242. https://doi.org/10.1016/J.YDBIO.2011.01.013

835 Kurusu M., A. Cording, M. Taniguchi, K. Menon, E. Suzuki, *et al.*, 2008 A Screen of Cell-Surface

836   Molecules Identifies Leucine-Rich Repeat Proteins as Key Mediators of Synaptic Target

837   Selection. Neuron 59: 972–985. https://doi.org/10.1016/J.NEURON.2008.07.037

838 Landis G. N., D. Bhole, and J. Tower, 2003 A search for doxycycline-dependent mutations that

839   increase Drosophila melanogaster life span identifies the VhaSFD, Sugar baby, filamin, fwd

840   and Cctlgenes. Genome Biol. 2003 42 4: 1–14. https://doi.org/10.1186/GB-2003-4-2-R8

841 Lavoy S., V. G. Chittoor-Vinod, C. Y. Chow, and I. Martin, 2018 Genetic Modifiers of

842   Neurodegeneration in a Drosophila Model of Parkinson's Disease. Genetics 209: 1345–

843   1356. https://doi.org/10.1534/genetics.118.301119

844 Lee G., and J. H. Park, 2004 Hemolymph Sugar Homeostasis and Starvation-Induced

845   Hyperactivity Affected by Genetic Manipulations of the Adipokinetic Hormone-Encoding

846   Gene in Drosophila melanogaster. Genetics 167: 311–323.

847   https://doi.org/10.1534/GENETICS.167.1.311

848 Li X., S. Zhang, G. Blander, J. Tse, M. Krieger, *et al.*, 2007 SIRT1 deacetylates and positively

849   regulates the nuclear receptor LXR. Mol. Cell 28: 91–106.

850   https://doi.org/10.1016/J.MOLCEL.2007.07.032

851 Lizák B., A. Szarka, Y. Kim, K. Choi, C. E. Németh, *et al.*, 2019 Glucose Transport and

852   Transporters in the Endomembranes. Int. J. Mol. Sci. 20.

853   https://doi.org/10.3390/IJMS20235898

854 Loubéry S., C. Seum, A. Moraleda, A. Daeden, M. Fürthauer, *et al.*, 2014 Uninflatable and

855   Notch Control the Targeting of Sara Endosomes during Asymmetric Division. Curr. Biol. 24:

856   2142–2148. https://doi.org/10.1016/J.CUB.2014.07.054

857 Lu J., S. J. Marygold, W. H. Gharib, and B. Suter, 2016 The aminoacyl-tRNA synthetases of

858   Drosophila melanogaster. https://doi.org/10.1080/19336934.2015.1101196 9: 53–61.

859   https://doi.org/10.1080/19336934.2015.1101196

860 Luo C.-W., E. M. Dewey, S. Sudo, J. Ewer, S. Y. Hsu, *et al.*, 2005 Bursicon, the insect cuticle-

861   hardening hormone, is a heterodimeric cystine knot protein that activates G protein-

862   coupled receptor LGR2. Proc. Natl. Acad. Sci. 102: 2820–2825.

863   https://doi.org/10.1073/PNAS.0409916102

864 Mackay T. F. C., S. Richards, E. A. Stone, A. Barbadilla, J. F. Ayroles, *et al.*, 2012 The

865   Drosophila melanogaster Genetic Reference Panel. Nature 482: 173–178.

866   https://doi.org/10.1038/nature10811

867 May C. E., A. Vaziri, Y. Q. Lin, O. Grushko, M. Khabiri, *et al.*, 2019 High Dietary Sugar

868   Reshapes Sweet Taste to Promote Feeding Behavior in Drosophila melanogaster. Cell

869   Rep. 27: 1675-1685.e7. https://doi.org/10.1016/J.CELREP.2019.04.027

870 McMullen E., A. Weiler, H. M. Becker, and S. Schirmeier, 2021 Plasticity of Carbohydrate

871   Transport at the Blood-Brain Barrier. Front. Behav. Neurosci. 0: 271.

872   https://doi.org/10.3389/FNBEH.2020.612430

873 Millington J. W., and E. J. Rideout, 2018 Sex differences in Drosophila development and

874   physiology. Curr. Opin. Physiol. 6: 46–56. https://doi.org/10.1016/J.COPHYS.2018.04.002

875 Montojo J., K. Zuberi, H. Rodriguez, F. Kazi, G. Wright, *et al.*, 2010 GeneMANIA Cytoscape

876   plugin: fast gene function predictions on the desktop. Bioinformatics 26: 2927–8.

877   https://doi.org/10.1093/bioinformatics/btq562

878 Nelson C. S., J. N. Beck, K. A. Wilson, E. R. Pilcher, P. Kapahi, *et al.*, 2016 Cross-phenotype

879   association tests uncover genes mediating nutrient response in Drosophila. BMC

880   Genomics 17. https://doi.org/10.1186/s12864-016-3137-9

881   Nogueiras R., K. M. Habegger, N. Chaudhary, B. Finan, A. S. Banks, *et al.*, 2012 Sirtuin 1 and

882   sirtuin 3: Physiological modulators of metabolism. Physiol. Rev. 92: 1479–1514.

883   https://doi.org/10.1152/physrev.00022.2011

884   Oas S. T., A. L. Bryantsev, and R. M. Cripps, 2014 Arrest is a regulator of fiber-specific

885   alternative splicing in the indirect flight muscles of Drosophila. J. Cell Biol. 206: 895–908.

886   https://doi.org/10.1083/JCB.201405058

887   Owusu-Ansah E., and N. Perrimon, 2014 Modeling metabolic homeostasis and nutrient sensing

888   in Drosophila: implications for aging and metabolic diseases. Dis. Model. Mech. 7: 343–

889   350. https://doi.org/10.1242/DMM.012989

890   Paik D., Y. G. Jang, Y. E. Lee, Y. N. Lee, R. Yamamoto, *et al.*, 2012 Misexpression screen

891   delineates novel genes controlling Drosophila lifespan. Mech. Ageing Dev. 133: 234–245.

892   https://doi.org/10.1016/J.MAD.2012.02.001

893   Palu R. A. S., and C. S. Thummel, 2016 Sir2 Acts through Hepatocyte Nuclear Factor 4 to

894   maintain insulin Signaling and Metabolic Homeostasis in Drosophila. PLoS Genet. 12: 1–

895   18. https://doi.org/10.1371/journal.pgen.1005978

896   Palu R. A. S., and C. Y. Chow, 2018 Baldspot/ELOVL6 is a conserved modifier of disease and

897   the ER stress response. PLoS Genet. 14. https://doi.org/10.1101/261206

898   Palu R. A. S., E. Ong, K. Stevens, S. Chung, K. G. Owings, *et al.*, 2019 Natural Genetic

899   Variation Screen in Drosophila Identifies Wnt Signaling, Mitochondrial Metabolism, and

900   Redox Homeostasis Genes as Modifiers of Apoptosis. G3 Genes|Genomes|Genetics 9:

901   g3.400722.2019. https://doi.org/10.1534/g3.119.400722

902   Palu R. A. S., H. M. Dalton, and C. Y. Chow, 2020 Decoupling of Apoptosis from Activation of

903   the ER Stress Response by the Drosophila Metallopeptidase superdeath. Genetics 214:

904   913–925. https://doi.org/10.1534/GENETICS.119.303004

905   Park J. W., K. Parisky, A. M. Celotto, R. A. Reenan, and B. R. Graveley, 2004 Identification of

906   alternative splicing regulators by RNA interference in Drosophila. Proc. Natl. Acad. Sci.

907   101: 15974–15979. https://doi.org/10.1073/PNAS.0407004101

908 Picard F., M. Kurtev, N. Chung, A. Topark-Ngarm, T. Senawong, *et al.*, 2004 Sirt1 promotes fat

909   mobilization in white adipocytes by repressing PPAR-gamma. Nature 429: 771–776.

910   https://doi.org/10.1038/NATURE02583

911 Prakash S., J. C. Caldwell, D. F. Eberl, and T. R. Clandinin, 2005 Drosophila N-cadherin

912   mediates an attractive interaction between photoreceptor axons and their targets. Nat.

913   Neurosci. 2005 84 8: 443–450. https://doi.org/10.1038/nn1415

914 Prisco G. Di, V. Cavaliere, D. Annoscia, P. Varricchio, E. Caprio, *et al.*, 2013 Neonicotinoid

915   clothianidin adversely affects insect immunity and promotes replication of a viral pathogen

916   in honey bees. Proc. Natl. Acad. Sci. 110: 18466–18471.

917   https://doi.org/10.1073/PNAS.1314923110

918 Queitsch C., K. D. Carlson, and S. Girirajan, 2012 Lessons from model organisms: phenotypic

919   robustness and missing heritability in complex disease. PLoS Genet 8: e1003041.

920   https://doi.org/10.1371/journal.pgen.1003041

921 Rabelink T. J., B. M. van den Berg, M. Garsen, G. Wang, M. Elkin, *et al.*, 2017 Heparanase:

922   roles in cell survival, extracellular matrix remodelling and the development of kidney

923   disease. Nat. Rev. Nephrol. 2017 134 13: 201–212. https://doi.org/10.1038/nrneph.2017.6

924 Rao Y., P. Pang, W. Ruan, D. Gunning, and S. L. Zipursky, 2000 brakeless is required for

925   photoreceptor growth-cone targeting in Drosophila. Proc. Natl. Acad. Sci. 97: 5966–5971.

926   https://doi.org/10.1073/PNAS.110135297

927 Reis T., M. R. Van Gilst, and I. K. Hariharan, 2010 A Buoyancy-Based Screen of Drosophila

928   Larvae for Fat-Storage Mutants Reveals a Role for Sir2 in Coupling Fat Storage to Nutrient

929   Availability, (E. Rulifson, Ed.). PLoS Genet. 6: e1001206.

930   https://doi.org/10.1371/journal.pgen.1001206

931 Rine J., and I. Herskowitz, 1987 Four Genes Responsible for a Position Effect on Expression

932   from HML and HMR in Saccharomyces cerevisiae. Genetics 116: 9.

933   Rodgers J. T., and P. Puigserver, 2007 Fasting-dependent glucose and lipid metabolic

934   response through hepatic sirtuin 1. Proc. Natl. Acad. Sci. U. S. A. 104: 12861–12866.

935   https://doi.org/10.1073/pnas.0702509104

936   Shannon P., A. Markiel, O. Ozier, N. S. Baliga, J. T. Wang, *et al.*, 2003 Cytoscape: a software

937   environment for integrated models of biomolecular interaction networks. Genome Res. 13:

938   2498–504. https://doi.org/10.1101/gr.1239303

939   Shlevkov E., and G. Morata, 2012 A dp53/JNK-dependant feedback amplification loop is

940   essential for the apoptotic response to stress in Drosophila. Cell Death Differ. 19: 451–460.

941   https://doi.org/10.1038/cdd.2011.113

942   Shore D., M. Squire, and K. A. Nasmyth, 1984 Characterization of two genes required for the

943   position-effect control of yeast mating-type genes. EMBO J. 3: 2817.

944   Sieber M. H., and C. S. Thummel, 2009 The DHR96 Nuclear Receptor Controls Triacylglycerol

945   Homeostasis in Drosophila. Cell Metab. 10: 481–490.

946   https://doi.org/10.1016/J.CMET.2009.10.010

947   Sivachenko A., H. B. Gordon, S. S. Kimball, E. J. Gavin, J. L. Bonkowsky, *et al.*, 2016

948   Neurodegeneration in a Drosophila model of adrenoleukodystrophy: the roles of the

949   Bubblegum and Double bubble acyl-CoA synthetases. Dis. Model. Mech. 9: 377–387.

950   https://doi.org/10.1242/DMM.022244

951   Somogyi K., B. Sipos, Z. Pénzes, and I. Andó, 2010 A conserved gene cluster as a putative

952   functional unit in insect innate immunity. FEBS Lett. 584: 4375–4378.

953   https://doi.org/10.1016/J.FEBSLET.2010.10.014

954   Spletter M. L., C. Barz, A. Yeroslaviz, C. Schönbauer, I. R. S. Ferreira, *et al.*, 2015 The RNA-

955   binding protein Arrest (Bruno) regulates alternative splicing to enable myofibril maturation

956   in Drosophila flight muscle. EMBO Rep. 16: 178–191.

957   https://doi.org/10.15252/EMBR.201439791

958   Subramanian A., P. Tamayo, V. K. Mootha, S. Mukherjee, B. L. Ebert, *et al.*, 2005 Gene set

959 enrichment analysis: a knowledge-based approach for interpreting genome-wide

960 expression profiles. Proc. Natl. Acad. Sci. U. S. A. 102: 15545–50.

961 https://doi.org/10.1073/pnas.0506580102

962 Talsness D. M., K. G. Owings, E. Coelho, G. Mercenne, J. M. Pleinis, *et al.*, 2020 A drosophila

963 screen identifies nkcc1 as a modifier of ngly1 deficiency. Elife 9: 1–22.

964 https://doi.org/10.7554/ELIFE.57831

965 Tennessen J. M., W. E. Barry, J. Cox, and C. S. Thummel, 2014 Methods for studying

966 metabolism in Drosophila. Methods 68: 105–115.

967 https://doi.org/10.1016/j.ymeth.2014.02.034

968 Udler M. S., M. I. McCarthy, J. C. Florez, and A. Mahajan, 2019 Genetic Risk Scores for

969 Diabetes Diagnosis and Precision Medicine. Endocr. Rev. 40: 1500–1520.

970 https://doi.org/10.1210/er.2019-00088

971 Wu H., and C. M. Ballantyne, 2020 Metabolic Inflammation and Insulin Resistance in Obesity.

972 Circ. Res. 126: 1549. https://doi.org/10.1161/CIRCRESAHA.119.315896

973 Yang J., X. Kong, M. Martins-Santos, G. Aleman, E. Chaco, *et al.*, 2009 Activation of SIRT1 by

974 resveratrol represses transcription of the gene for the cytosolic form of

975 phosphoenolpyruvate carboxykinase (GTP) by deacetylating hepatic nuclear factor 4alpha.

976 J. Biol. Chem. 284: 27042–27053. https://doi.org/10.1074/JBC.M109.047340

977 Zhao Y., J. Wei, X. Hou, H. Liu, F. Guo, *et al.*, 2017 SIRT1 rs10823108 and FOXO1

978 rs17446614 responsible for genetic susceptibility to diabetic nephropathy. Sci. Reports

979 2017 71 7: 1–9. https://doi.org/10.1038/s41598-017-10612-7

980 Zhou X., and M. Stephens, 2012 Genome-wide efficient mixed-model analysis for association

981 studies. Nat. Genet. 44: 821–4. https://doi.org/10.1038/ng.2310

982 Zhou X., C. J. Guo, H. H. Hu, J. Zhong, Q. Sun, *et al.*, 2019 Drosophila CTP synthase can form

983 distinct substrate- and product-bound filaments. J. Genet. Genomics 46: 537–545.

984 https://doi.org/10.1016/J.JGG.2019.11.006

985 Zillikens M. C., J. B. J. van Meurs, F. Rivadeneira, N. Amin, A. Hofman, *et al.*, 2009 SIRT1

986   Genetic Variation Is Related to BMI and Risk of Obesity. Diabetes 58: 2828–2834.

987   https://doi.org/10.2337/DB09-0536

988

989   **FIGURE LEGENDS**

990 **Figure 1. Glucose levels vary under a variety of environmental conditions.**

991 Glucose levels were measured in three samples for each of 30-36 strains under one of the

992 indicated conditions: one week of adult age and fed ad libitum (N = 30 strains, P = 1.87E-05)

993 (**A**), one week of adult age and fasted for 12-13 hours (N = 30 strains, P = 0.0194) (**B**), two

994 weeks of adult age and fed ad libitum (N = 30 strains, P = 0.0103) (**C**), and two weeks of adult

995 age and fasted for 12-13 hours (N = 36 strains, P = 1.95E-05) (**D**). Mean glucose concentrations

996 are indicated, with error bars indicating standard deviation. DGRP strain or RAL numbers are

997 indicated along the X-axis. P-values were calculated using one-way ANOVA incorporating all

998 individual measurements comparing DGRP strain with glucose concentration. Adult flies were

999 collected within 2-3 days after eclosion from the pupal case and aged to the indicated time

1000 points. * P < 0.05, **** P < 5E-05.

1001

1002 **Figure 2. Glucose levels are significantly affected by genetic background.**

1003 Glucose levels were measured in three samples for each of 185 strains at two weeks of age

1004 after a 12 hour fast. Adult flies were collected within 2-3 days after eclosion from the pupal case

1005 and aged an additional 9-11 days prior to fasting (11-14 days post-eclosion). Flies were

1006 collected after the overnight fast at 12-15 days post-eclosion. Mean glucose concentrations are

1007 indicated, with error bars indicating standard deviation. P-values were calculated using one-way

1008 ANOVA incorporating all individual measurements comparing DGRP strain with glucose

1009 concentration (P < 2E-16).

1010

1011 **Figure 3. Immune responses, neuronal function, and basic metabolic processes are**

1012 **overrepresented in GWA candidate modifiers of hyperglycemia.**

1013 (**A**) *R4>Sirt1i* modifier network, as plotted by the GeneMANIA plugin in Cytoscape (Shannon *et*

1014 *al.* 2003; Montojo *et al.* 2010). Significant candidate modifiers are indicated in red, with physical

1015 interactions indicated by connecting red lines. Thicker lines indicate stronger evidence for the

1016 interaction. Encircled genes share common pathways or functions. Interacting genes outside of

1017 the candidate modifier list are indicated in gray. (**B**) Top 20 significant ontological categories as

1018 identified by GSEA. Categories are arranged from most significant on top to least significant

1019 along the y-axis. P-values are indicated by red-to-blue gradient, with red the lowest p-values

1020 and blue the highest P-values. Enrichment score (ES) for each category is plotted along the x-

1021 axis. Gene number identified in each category is indicated by dot size.

1022

1023 **Figure 4. Loss of candidate gene expression suppresses hyperglycemia in the R4>Sirt1i**

1024 **model**

1025 RNAi against candidate modifiers was expressed under the control of *R4-GAL4* in the *R4>Sirt1i*

1026 model. Glucose level for each sample was normalized to the levels in a genetically matched

1027 control line crossed into the *R4-Sirt1* line. Average *R4>Sirt1i* control glucose levels after

1028 normalization are indicated by a dotted line at 1.0, with standard deviation highlighted by the gray

1029 box. Whole fly glucose concentration was quantified for N = 4-5 samples per strain, each

1030 consisting of 5 flies and individually plotted along the y-axis. Knockdown of *CG4168, CG5888*, or

1031 *uif* significantly reduces glucose concentrations in the *R4>Sirt1i* model of hyperglycemia

1032 compared to controls (blue). Loss of *CTPSyn* does not significantly alter glucose levels, but a

1033 trending decrease in glucose levels were observed in several independent RNAi strains (light

1034 blue, data not shown). Loss of *smt3*, *ilp5*, *snRNP-U1-70k*, *CG10265*, *CG15803*, *Roe*, *CG34353*,

1035 *CadN2*, *CG43897*, *CG3407*, *dsxc73A*, or *bgm* do not produce a significant effect (dark gray). P-

1036   values were calculated using one-way ANOVA followed by Dunnett's multiple testing correction.

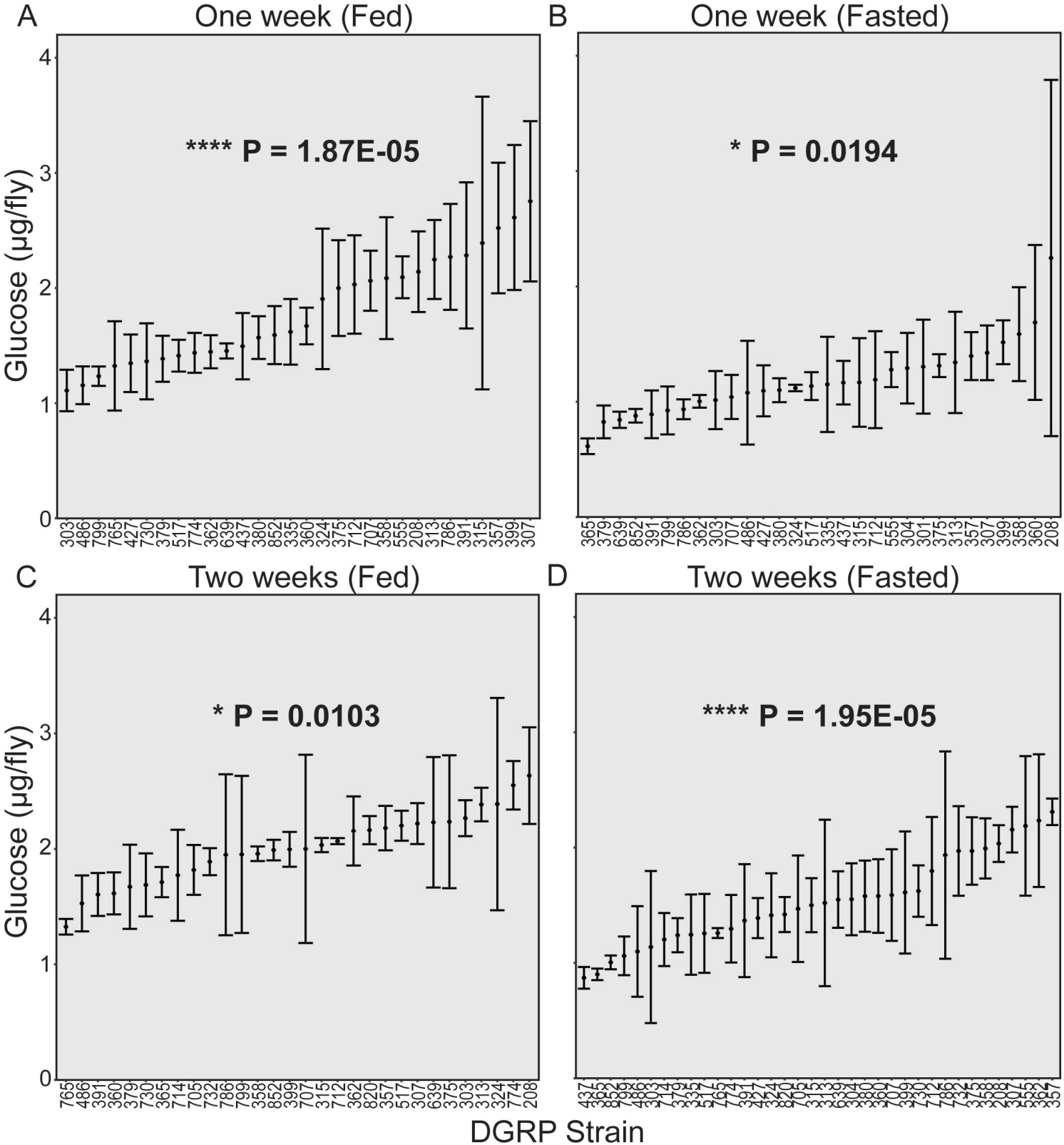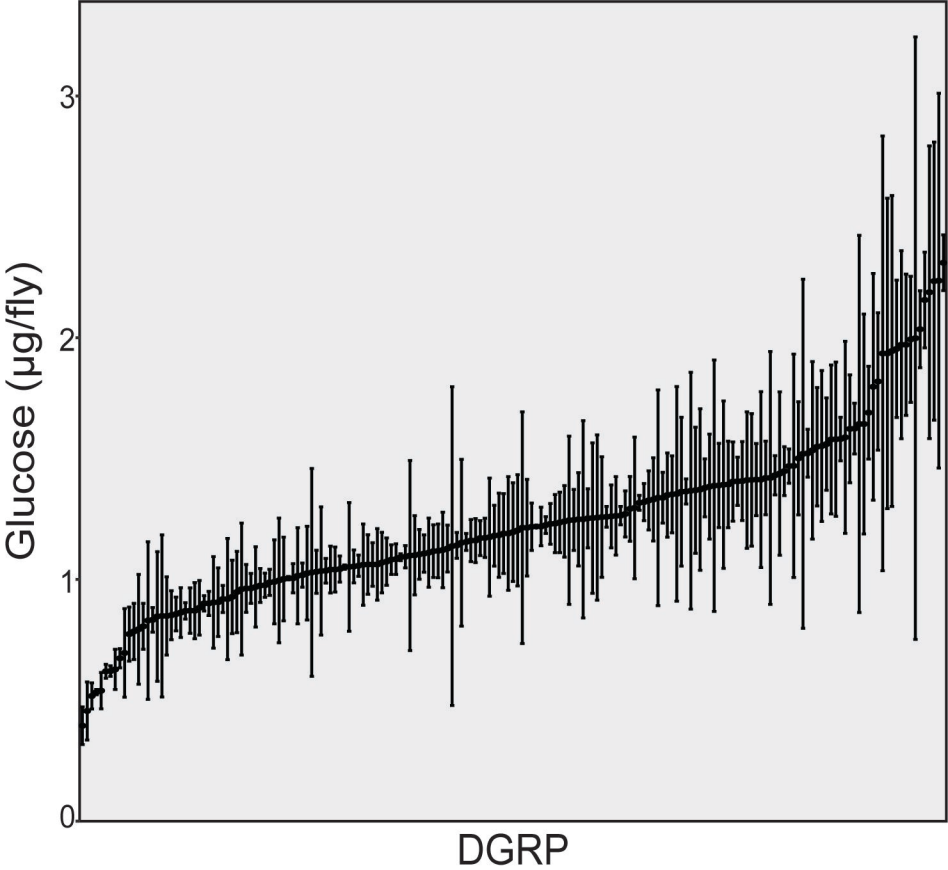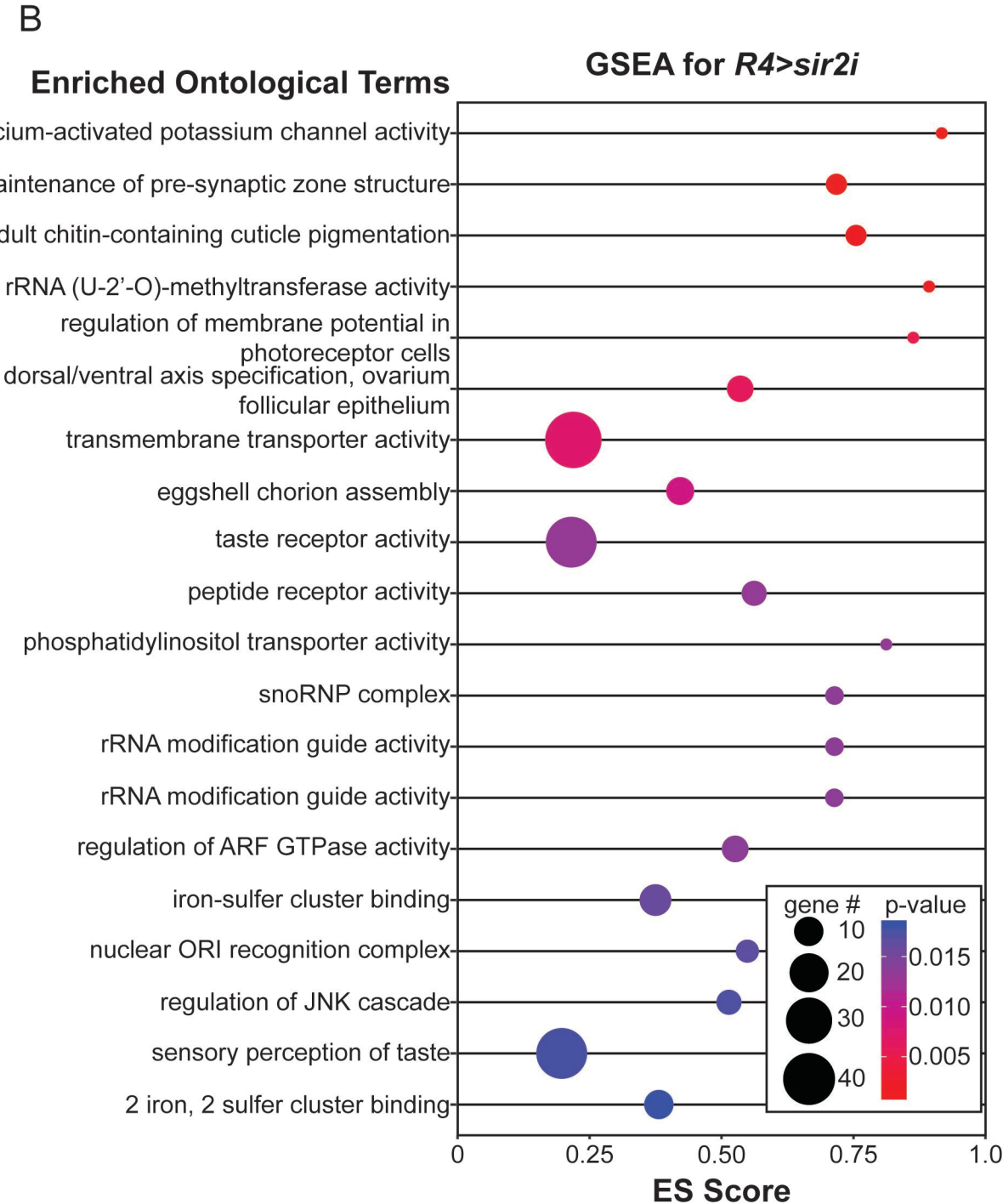1037   * $P < 0.05$, *** $P < 0.001$.

Figure 1.

Figure 2

Figure 3

Figure 4